

## Determination of the Diffusivity of *n*-Pentane in Polystyrene Bead Foam

D. J. FOSSEY and C. H. SMITH, *Materials Engineering, Bendix Corporation, Kansas City Division, Kansas City, Missouri 64141*

### Synopsis

The amount of residual *n*-pentane in expandable polystyrene bead foam (PSBF) has an effect on the strength and dimensional stability of the foam. Data were needed to determine how fast the residual *n*-pentane could be removed to enhance the properties of PSBF. An experiment was designed to determine the diffusivity of *n*-pentane through PSBF at various temperatures. Mathematical models based on the appropriate diffusion differential equations were then used to predict *n*-pentane concentrations in cylinders of PSBF. The diffusivity of *n*-pentane through PSBF was found to have a magnitude of  $1 \times 10^{-8}$  to  $1 \times 10^{-6}$  cm<sup>2</sup>/sec and to vary with temperature, foam density, *n*-pentane concentration, and foam structure.

### INTRODUCTION

Polystyrene bead foam is manufactured from solid expandable polystyrene beads containing 5% to 6% *n*-pentane dissolved in the polymer. The *n*-pentane becomes a blowing agent and plasticizer at high temperatures, which provides the mechanism by which the beads can be fused. Approximately 40% of the original *n*-pentane content remains in the foam after the molding operation. This high *n*-pentane residue is due to the size and density of the parts being molded.

This residual *n*-pentane plasticizes the polystyrene foam, reducing its tensile strength and maximum usable temperature. As the foam ages, the *n*-pentane diffuses out and the foam becomes stronger and smaller and achieves a higher temperature capability.<sup>1</sup> Thus, it is desirable to know the diffusivity of *n*-pentane through polystyrene bead foam to predict the time required for polystyrene foam parts to age enough to acquire the design properties.

An experiment was designed to determine the diffusivity of *n*-pentane through 1-in.-thick (25.4 mm) slabs of polystyrene foam from weight loss data at various temperatures. The weight loss data were then evaluated, using the appropriate differential equations, to determine the diffusivity. This permitted prediction of the aging time for removal of *n*-pentane from a polystyrene foam part.

A search of the literature revealed that the theory of the diffusion of gases through polymers is still in the development stages. This is par-

ticularly true in the temperature range near the glass transition temperature of the polymer. A wide variety of polymer-gas systems have been investigated. However, considering the large number of polymers available, there is still a lot of work to be done to develop more general theories of diffusion in polymers. Furthermore, very little work has been published on polymeric foam-gas systems. Polymeric foams have been increasingly used as engineering material in recent years. Many of the applications of polymer foams require the knowledge of gas diffusion in and out of the foam, such as the increase in the thermal conductivity of polyurethane foam when air diffuses into the cells.

Thus, there is a great need for a better understanding of the mechanism of gas diffusion in polymeric foams. There is a need also for experimental data for the diffusivity of gases in polymeric foams.

### EXPERIMENTAL DESIGN

Diffusivity is defined by Fick's law of diffusion<sup>2</sup> as

$$F = D \frac{dc}{dt} \quad (1)$$

where  $F$  is a driving force, such as a concentration gradient;  $D$  is the diffusivity or diffusion coefficient; and  $dc/dt$  is the change in concentration with respect to time. The diffusivity is considered to be a proportionality coefficient that must be determined experimentally.

The diffusion of a gas in closed-cell polymeric foam is very complicated, more so than diffusion in a solid polymeric film. Considering a solid polymeric film, the diffusivity may be a constant (independent of time and concentration) or a variable with respect to concentration and time. In polymeric foam systems, there are the additional variables of cell size, wall thickness, density, and porosity. Another complication in the polystyrene-*n*-pentane system is that the *n*-pentane is located in both the vapor phase and solid phase of the foam. The foam may be regarded as a multi-layer laminate of thin polymer films and thick gas layers. The *n*-pentane has to dissolve on one side of a polymer film, diffuse through the film, evaporate, and then diffuse through the gas layer. This process is repeated many times. The dependence of the diffusivity on temperature is well documented in the literature, which states that the logarithm of the diffusivity varies linearly with the inverse of the absolute temperature,  $1/T$ .

The approach used to determine the diffusivity of *n*-pentane in polystyrene bead foam was to make the following simplifying assumptions to obtain an ideal model to which the appropriate differential equations describing diffusion of gases in a solid could be applied:

1. The diffusivity is independent of concentration and time.
2. The foam is a homogeneous material with constant cell size and cell wall thickness throughout the foam specimen for a given foam density.
3. The porosity does not vary from sample to sample.

4. The initial pentane concentration is uniform throughout the foam specimen and the air surrounding the foam specimen has zero pentane concentration at all times.

By selecting an appropriate sample configuration, a 6-in. by 6-in. by 1-in. (152-mm by 152-mm by 25.4-mm) specimen, the problem was reduced to the determination of the one-dimensional diffusion of *n*-pentane in the foam by weight loss measurements. The experimental procedure was designed to evaluate the effect of density and temperature on the diffusivity and to obtain the necessary data to prove or disprove the assumptions.

### THEORETICAL APPROACH

The differential equations that describe the diffusion of a gas through a solid have been solved and are in the literature.<sup>2</sup> The resulting equation for the experimental conditions to be discussed is as follows:

$$\frac{M_t}{M_\infty} = 1 - \sum_{n=0}^{\infty} \frac{8}{(2n+1)^2 \pi^2} \exp\left\{\frac{-D(2n+1)^2 \pi^2 t}{4L^2}\right\}, \quad n = 1, 2, 3, \dots \quad (2)$$

where  $M_t$  = total amount of diffusing substance that has diffused out of the specimen by the time  $t$ , in grams;  $M_\infty$  = total amount of diffusing substance leaving the specimen as  $t$  approaches infinity, in grams;  $D$  = diffusivity, in  $\text{cm}^2/\text{sec}$ ;  $L$  = half-thickness of foam specimen, in cm; and  $t$  = time, in seconds. Equation (2) can be simplified to the following equation:

$$E = \frac{C_t}{C_0} = 8 \exp(0.25) \sum_{N=1}^{\infty} \frac{1}{p} \exp(-PT), \quad N = 1, 3, 5, \dots \quad (3)$$

where  $E$  = fraction of initial *n*-pentane remaining in foam at time  $t$ , dimensionless;  $C_t/C_0 = 1 - (M_t/M_\infty)$ ;  $C_t$  = average *n*-pentane concentration at time  $t$ , in grams;  $C_0$  = initial *n*-pentane concentration, in grams;  $P = N^2 \pi^2$ , dimensionless;  $T = Dt/L^2$  relative time unit, dimensionless; and  $N = 2n + 1$ , dimensionless.

To determine the diffusivity from eq. (3), the ratio  $C_t/C_0$  can be determined experimentally at various times by weight loss measurements. An iteration process can be used to calculate  $C_t/C_0$  from the right member of eq. (3) for assumed values of  $T$  and to compare to the experimentally determined  $C_t/C_0$  for the same period. The value of  $D$  can be calculated from relationship  $T = Dt/L^2$ . By so determining the diffusivity over a series of time increments, one can obtain its dependence on time and the *n*-pentane concentration,  $C_t$ .

The diffusivity, once determined, can be used to predict the average *n*-pentane concentration in a foam of a known size and shape at any given time when the foam is aged at constant temperature. The method used was developed by Treybal.<sup>3</sup> Figure 1 was produced from data presented by Treybal and shows the relationship between  $C_t/C_0$  and the relative time unit,  $T$ , for an infinite slab and an infinite cylinder.

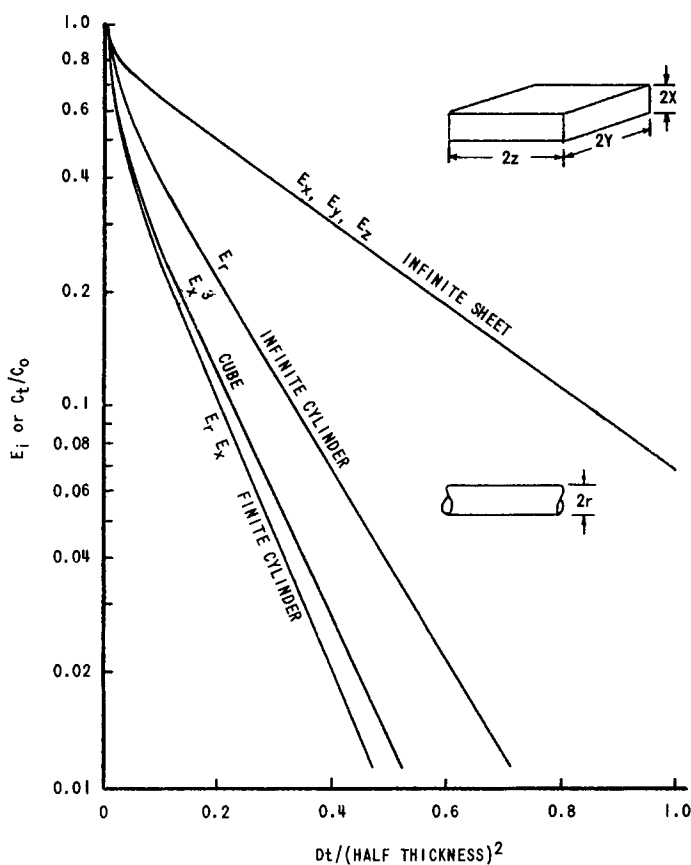


Fig. 1. Unsteady-state diffusion.

To computerize Treybal's data, equations describing the infinite cylinder and slab were determined.

For an infinite slab:

$$E_s = C_t/C_0 = 0.75 \exp(-2.5T_s) - 0.25 \exp(-3.91T_s^{0.48}). \quad (4)$$

For an infinite cylinder:

$$E_c = C_t/C_0 = \exp(-5.015T_c^{0.715}) \quad (5)$$

where  $T_s = Dt/L^2$ , dimensionless;  $L = \frac{1}{2}$  thickness of slab, in cm;  $T_c = Dt/R^2$ , dimensionless; and  $R =$  radius of cylinder, in cm.

As part of Treybal's theory, the product of  $E_s$  and  $E_c$  gives the ratio  $C_t/C_0$  or  $E$  for a finite cylinder; or, by cubing  $E_s$ ,  $E$  may be obtained for a cube. Thus,  $E$  can be calculated at any given time for a finite cylinder or cube of foam with known dimensions. The average concentration  $C_t$  after time  $t$  can then be calculated for a known  $C_0$ . These relationships were determined and are also given in Figure 1. Equations determined to fit these curves are as follows.

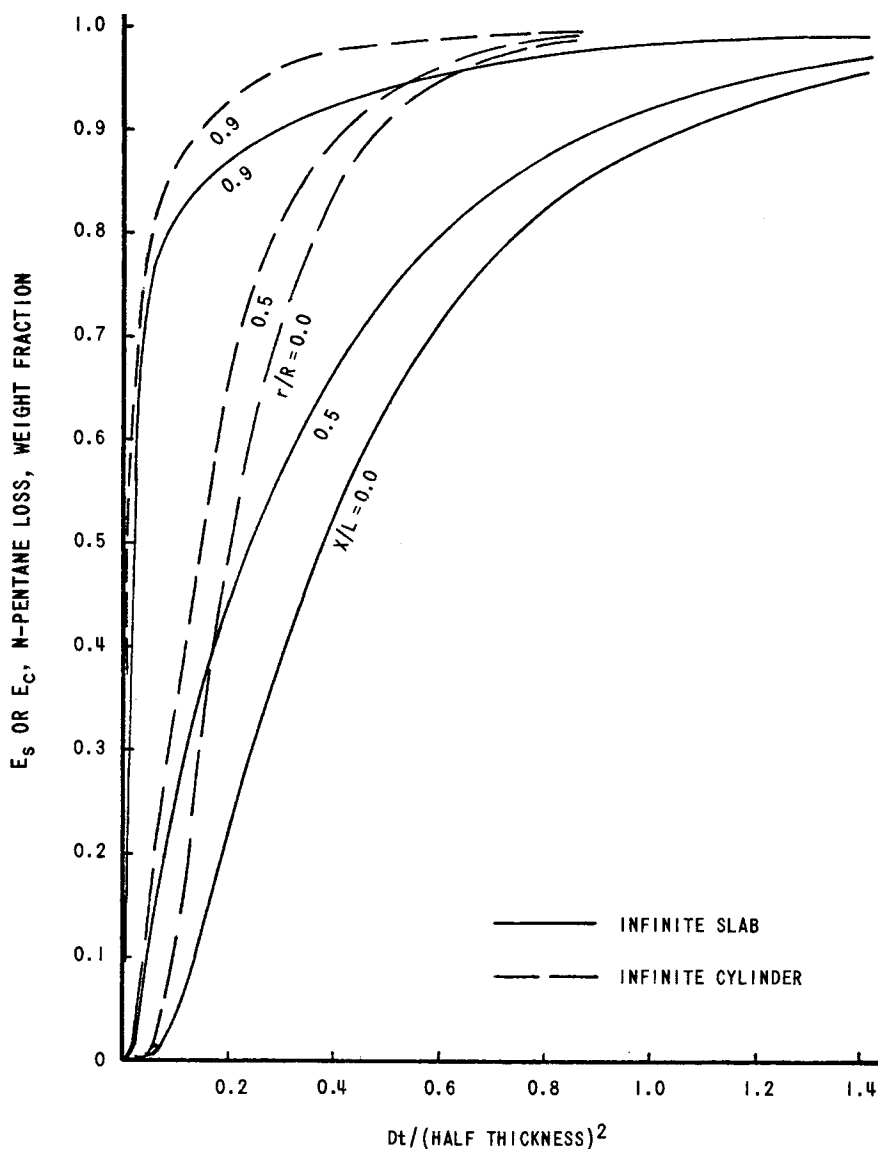


Fig. 2. Unsteady-state diffusion as a function of location.

For a finite cylinder:

$$E = \exp(-6.487T^{0.665}). \quad (6)$$

For a cube:

$$E = 0.90 \exp(-6.03T^{0.686}). \quad (7)$$

The *n*-pentane concentration at a given position within a finite cylinder may also be determined. The method used involves determining the equations for the curves at the desired locations,  $X/L$  and  $r/R$ . Figure 2

shows the relationship between  $E$  and  $T$  at constant  $X/L$  and  $r/R$  values of 0.0, 0.5, and 0.9 for finite slabs and cylinders.

The variables  $X$  and  $r$  are the distances from the geometric center of the slab or cylinder to the point of interest. These curves were determined from the three  $X/L$  and  $r/R$  ratios mentioned from a graph given by Crank and the equations describing these curves were determined to be as follows<sup>2</sup>:

$$E_{s_{0.0}} = 1.175 \exp(-2.42T_s^{1.08}) - 0.175 \exp(-68.97T_s^{0.382}) \quad (8)$$

$$E_{s_{0.5}} = 1.1 \exp(-2.58T_s^{0.83}); T_s > 0.02 \quad (9)$$

$$E_{s_{0.9}} = \exp(-4.2 T_s^{0.38}); T_s > 0.01 \quad (10)$$

$$E_{c_{0.0}} = 1.35 \exp(-5.75T_c^{1.09}) - 0.35 \exp(-62.2T_c^{1.3}) \quad (11)$$

$$E_{c_{0.5}} = 1.2 \exp(-5.65T_c^{0.41}); T_c > 0.03 \quad (12)$$

$$E_{c_{0.9}} = \exp(-5.62T_c^{0.43}), T_c > 0.01. \quad (13)$$

The value of  $E$  or  $C_i/C_0$  for a given point in the cylinder is the product of  $E_{s_i}$  and  $E_{c_j}$ , which are evaluated at the given time, position, and nine points in one quarter of a cylinder and which, at a desired aging time, can be predicted. Computer programs were written to evaluate these equations. A similar approach can be used to determine the local  $n$ -pentane concentration in a cube by taking the appropriate products of  $E_{s_i}$ .

## EXPERIMENTAL PROCEDURE

Two foam densities and four aging temperatures were used in this investigation: foam densities 0.05 and 0.10 gm/cc; and aging temperatures 77°F (25°C), 120°F (49°C), 150°F (66°C), and 170°F (77°C). Twelve 6-in. by 6-in. by 1.5-in. foam specimens for each of the two densities were removed from a 1.5-in.-thick slab that had been cut radially from a large cylinder 42 in. (1.06 m) in diameter by 30 in. (0.760 m) high. Their original location is shown in Figure 3. The specimens were then machined to 1.0 in. by 6 in. by 6 in. The weights and dimensions of each specimen were then recorded before and after sealing the four 1-in. wide surfaces with an epoxy adhesive and aluminum foil. The specimens were allowed to remain at room temperature for three days and were then weighed again before they were placed in air-circulating ovens at the specified temperatures for each sample. Periodically, the specimens were removed from the oven, cooled for 2 hr, and weighed. They were then returned to the oven for additional aging. The specimens aged at room temperature of 75° to 80°F (24° to 27°C) were also periodically weighed. After approximately two months, the aging tests were terminated.

When the specimens were removed from the oven for the last time, their increase in weight was monitored until it became constant. This procedure, which took two to three days, was used to determine the amount of air loss by expansion when the samples were hot. The specimens were

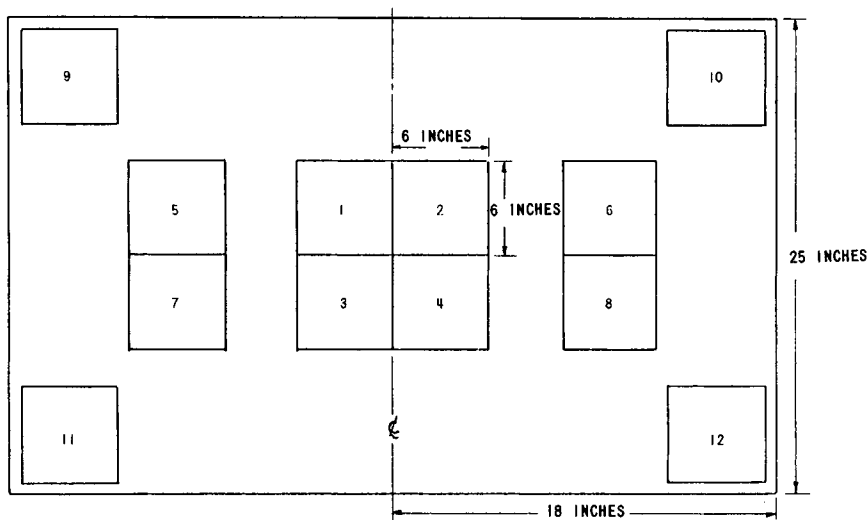


Fig. 3. Location of specimen removal from foam cylinder.

then heated to 302°F (150°C) for 10 min to remove any residual volatiles and to determine the initial weight of the polystyrene resin in each specimen. Allowances were made for the low ends in the polymer. Low ends are primarily dimers and trimers of styrene that are driven off at 302°F (150°C), the amount being determined by heating the raw stock material (without *n*-pentane) at 302°F (150°C) for 30 min. Additional tests were made to determine the approximate weight loss of the epoxy adhesive during the aging period at the elevated temperature and during the 302°F (150°C) drying cycle.

### TREATMENT OF EXPERIMENTAL RESULTS

The procedure for determining the weight loss of the foam specimens was straightforward. However, in determining the average residual *n*-pentane in the specimens at the time of each weighing, a correction to the recorded weights must be made to account for the loss of air, adhesive, and low ends during the heat-aging periods. These corrections were determined by the methods described in the preceding section. The average per cent residual *n*-pentane at each weighing was calculated, based on the original weight of the polymer in the foam specimen. The following equation was used:

$$C_t = (W_t - W_p)/W_p \quad (14)$$

where  $C_t$  = average *n*-pentane content at time  $t$ , weight fraction;  $W_p$  = weight of base polymer in the foam specimen, in grams; and  $W_t$  = corrected weight of the foam specimen at time  $t$ , in grams. The initial specimen weight,  $W$ , was determined at  $t = 0$ . Thus,  $C_0 = (W_0 - W_p)/$

$W_p$ . A programmable calculator (Friden Model 1151) was used to perform these calculations.

The average *n*-pentane concentrations were then used to calculate the diffusivity *D*, using the mathematics that had been developed. Since there were variations in the foam density from specimen to specimen, the diffusivity values were normalized linearly to the nominal densities of 0.05 and 0.10 g/cm<sup>3</sup> to reduce the effect of small density variations on the diffusivity.

### DISCUSSION OF RESULTS

From the experimental results, it can be seen that the assumptions made to simplify the diffusion problem were not completely justified. How-

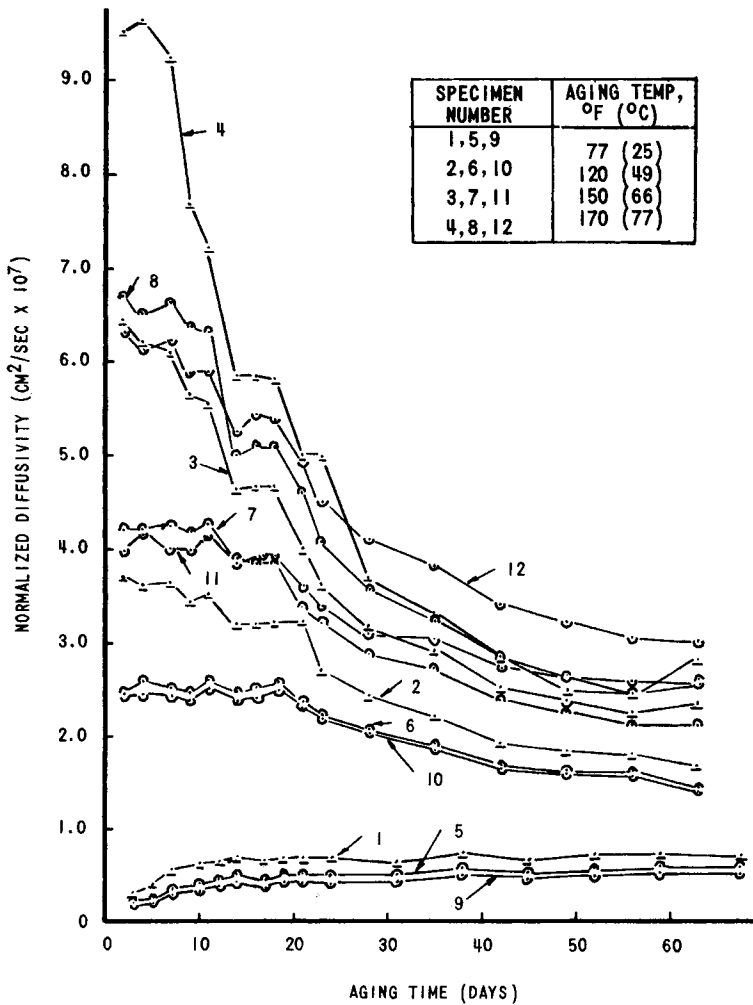


Fig. 4. Experimental diffusivity vs. aging time for 0.05 g/cm<sup>3</sup> foam.



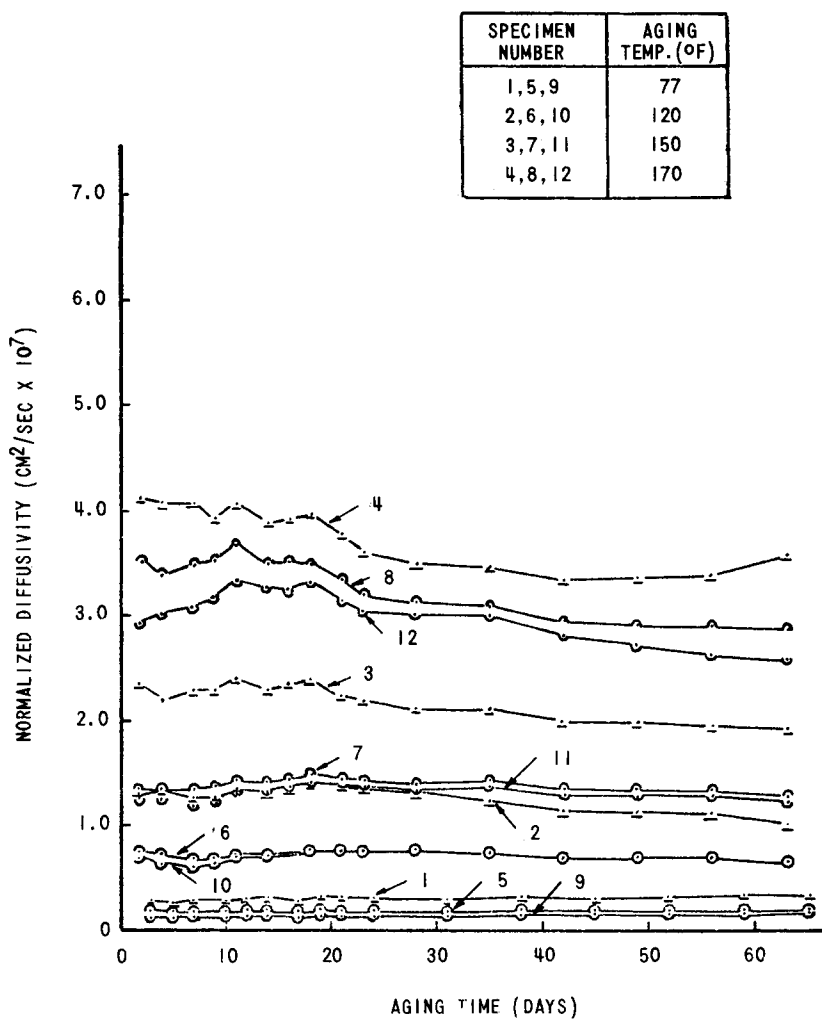


Fig. 5. Experimental diffusivity vs. aging time for 0.1 g/cm<sup>3</sup> foam.

ever, by using the simplified model, some usable data and conclusions were obtained.

Figures 4 and 5 show the normalized diffusivity values plotted versus the aging time for each specimen. From these figures, the *n*-pentane diffusivity for both densities was found to be essentially independent of aging time at room temperature. At elevated temperatures, the diffusivity became dependent upon aging time: the higher the temperature, the greater the dependence. The diffusivity decreased with increasing time and increased with increasing temperature. Some of the scatter in the data points shown in Figures 4 and 5 may be the result of air and moisture diffusing in and out of the foam. The relative humidity of the laboratory

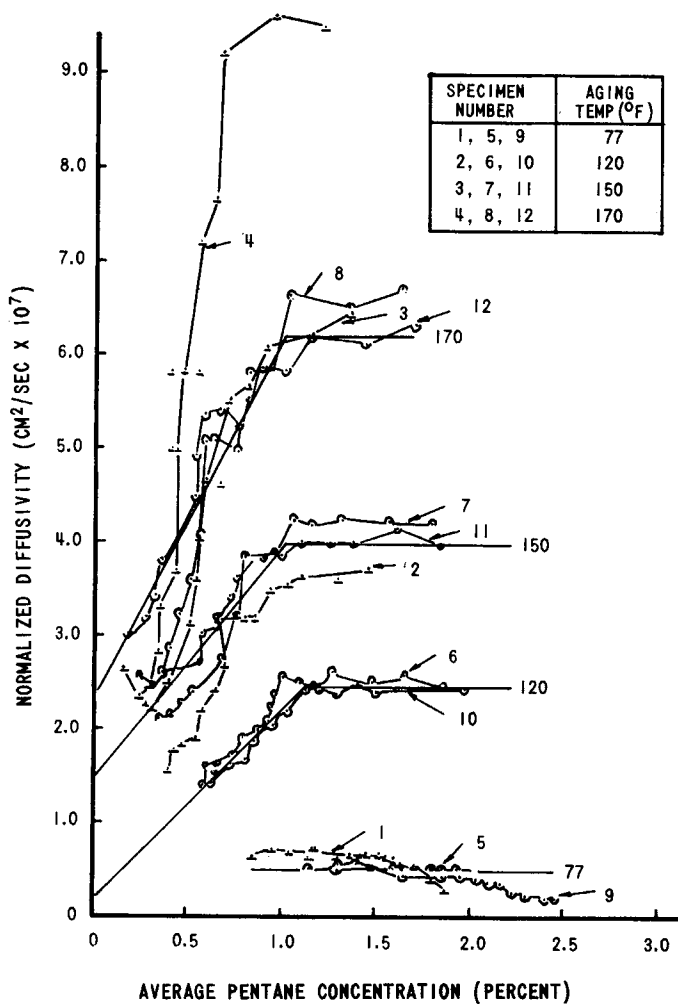


Fig. 6. Diffusivity vs. aging average concentration for 0.05 g/cm<sup>3</sup> foam.

in which the specimens were aged and weighed was not controlled and may have varied from 20% to 60%.

The dependence of the diffusivity on the *n*-pentane concentration was determined by plotting the average *n*-pentane concentration against the corresponding normalized diffusivity, as shown in Figures 6 and 7. When plotted in this manner, the data indicated that the diffusivity changed from concentration dependent at *n*-pentane concentrations below about 1% to concentration independent at concentrations above 1%.

The exact *n*-pentane concentration at which this transition takes place appears to decrease with increasing temperature and to be slightly lower for the 0.10 g/cm<sup>3</sup> foam. It is also postulated that the room temperature 77°F (25°C) aged specimens, both 0.05 and 0.10 g/cm<sup>3</sup>, were not aged long enough to show this transition from concentration independent to con-

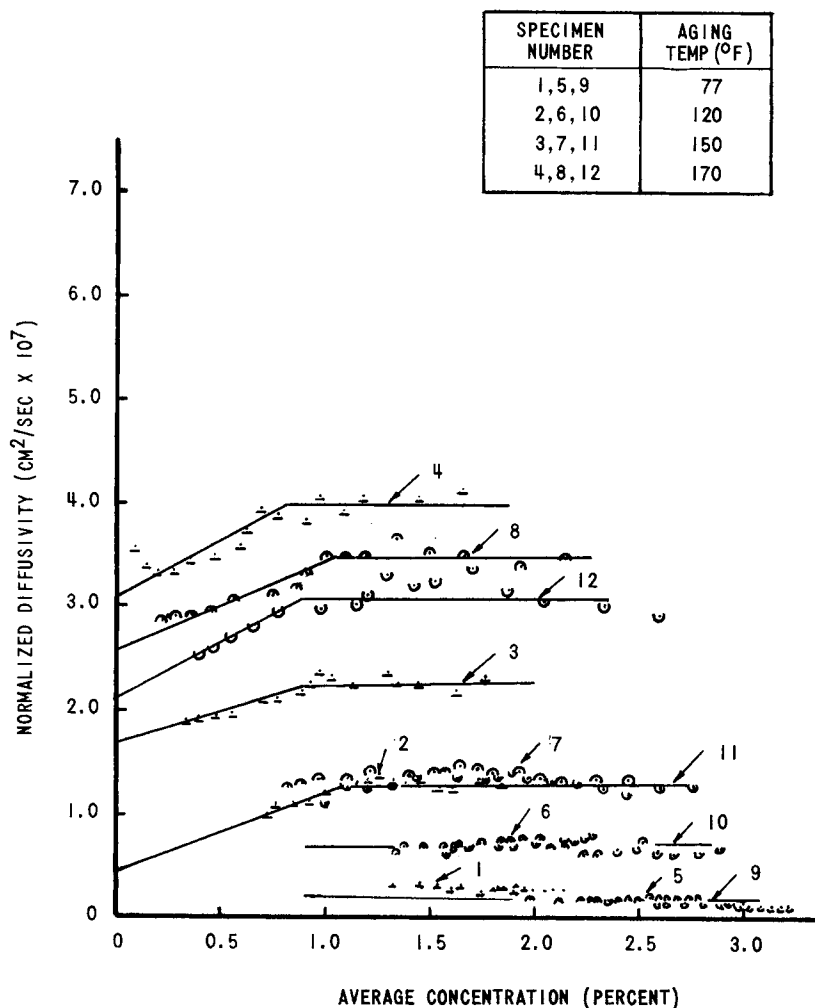


Fig. 7. Diffusivity vs. average concentration for 0.01 g/cm<sup>3</sup> foam.

centration dependent. Some of the 0.10 g/cm<sup>3</sup> foam specimens aged at 120°F (59°C) and 150°F (66°C) also may not have been aged long enough to pass this transition point. Equations for the lines through the data points for the edge specimens (9, 10, 11, and 12) were determined and are presented in Table I. These equations give the diffusivity as a function of *n*-pentane concentration.

The temperature dependence of diffusivity can be seen in Figures 8 and 9. These figures were constructed by obtaining diffusivity values at the indicated temperature and *n*-pentane concentrations from Figures 6 and 7 for the specimens taken from the edge of the foam cylinder. These data appeared to follow the Arrhenius relationship,  $\log D'$  versus  $1/T$ , within experimental error.

TABLE I  
Diffusivity as a Function of Average Concentration for  
Specimen Removed from Edge of Cylinder

Temp., °F(°C)	Equation $D = D(C)$ , <sup>a</sup> cm <sup>2</sup> /sec	Range of concentration, weight fraction
	Foam Density: 0.05 g/cm <sup>3</sup>	
77 (25)	$D = 5 \times 10^{-8}$	all
120 (49)	$D = 2.5 \times 10^{-7}$	$C_i > 0.011$
	$D = 2.0 \times 10^{-8} + 2.3C_i \times 10^{-6}$	$C_i < 0.011$
150 (66)	$D = 4.0 \times 10^{-7}$	$C_i > 0.010$
	$D = 1.5 \times 10^{-7} + 2.5C_i \times 10^{-6}$	$C_i < 0.010$
170 (77)	$D = 6.2 \times 10^{-7}$	$C_i > 0.010$
	$D = 2.3 \times 10^{-7} + 3.9C_i \times 10^{-6}$	$C_i < 0.010$
	Foam Density: 0.10 g/cm <sup>3</sup>	
77 (25)	$D = 2 \times 10^{-8}$	all
120 (49)	$D = 7 \times 10^{-8}$	all
150 (66)	$D = 1.3 \times 10^{-7}$	$C_i > 0.011$
	$D = 5 \times 10^{-8} + 7.3C_i \times 10^{-6}$	$C_i < 0.011$
170 (77)	$D = 3.1 \times 10^{-7}$	$C_i > 0.009$
	$D = 2.1 \times 10^{-7} + 1.1C_i \times 10^{-6}$	$C_i < 0.009$

<sup>a</sup>  $C_i$  dimensions are weight fraction.

TABLE II  
Arrhenius-Type Relationship Between Diffusivity, Activation Energy,  
and Temperature at Different Levels of *n*-Pentane Concentration

Foam density, g/cm <sup>3</sup>	<i>n</i> -Pentane concentration, %	Arrhenius equation $D = D_0 \exp(\Delta E/RT)$
0.05	>1.0	$D = 2.39 \exp(-9500/RT)$
0.05	0.5	$D = 1.98 \exp(-9650/RT)$
0.05	0.25	$D = 13.5 \exp(-11,000/RT)$
0.05	0.0	$D = 48,900 \exp(-16,360/RT)$
0.10	>1.0	$D = 1.25 \exp(-10,040/RT)$
0.10	0.5	$D = 5.2 \times 10^8 \exp(-22,170/RT)$
0.10	0.25	$D = 1.5 \times 10^{11} \exp(-25,830/RT)$
0.10	0.0	$D = 4.7 \times 10^{13} \exp(-29,520/RT)$

A computer program was written to determine the equations which fit two points on the straight lines in Figures 8 and 9. These equations are of the Arrhenius form,  $D = D_0 \exp(\Delta E/RT)$ , and are given in Table II, where  $D_0$  is an arbitrary constant, in cm<sup>2</sup>/sec;  $\Delta E$  is the activation energy, in cal/g·mole;  $R$  is the ideal gas constant, in 1.987 cal/g·mole·°K; and  $T$  is the absolute temperature, °K.

As can be seen from these equations, the values representing  $\Delta E/R$  increased with decreasing concentration of *n*-pentane, as would be expected with decreasing diffusivity values.

The assumption that the foam was of uniform cell size and wall thickness throughout the billet appeared invalid. Returning to Figures 6 and 7, it is

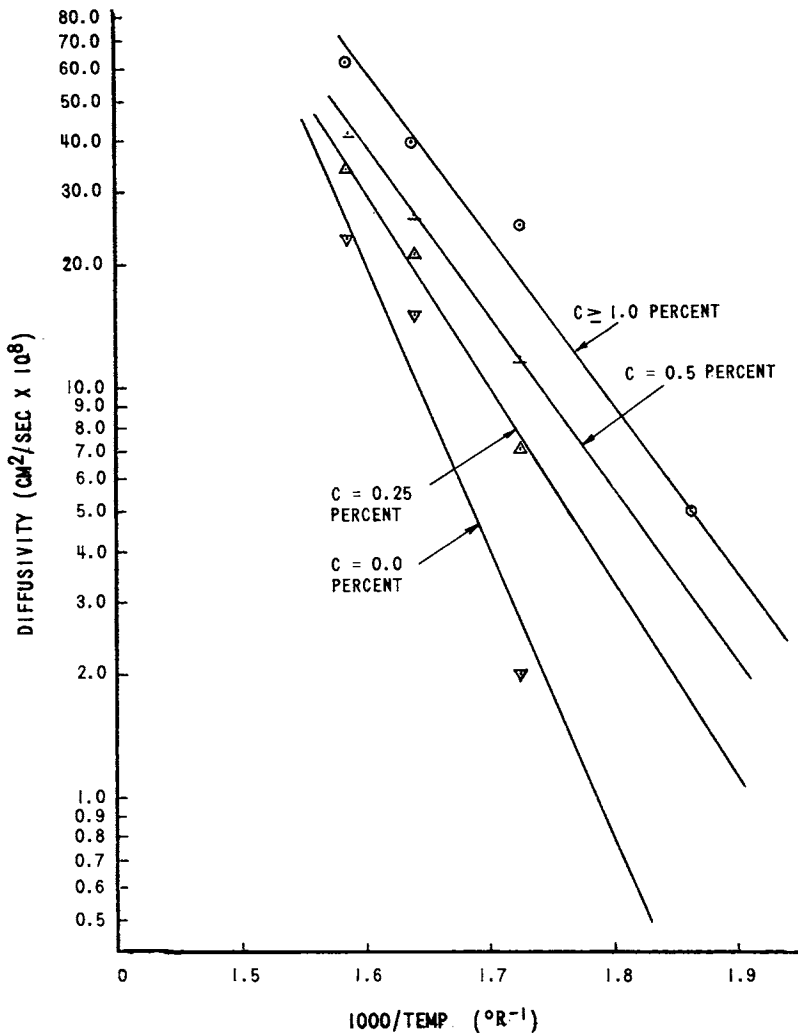


Fig. 8. Diffusivity as a function of temperature and concentration in 0.05 g/cm<sup>3</sup> foam.

noted that, in each group of specimens aged at each of the indicated temperatures, the specimens that were removed from the center of the billets had a higher diffusivity than the corresponding specimens removed from the other two locations in the billets. It is theorized that the center specimen has a high diffusivity because of higher open cell content (porosity) or thinner cell walls in the center of the billet than in the outer regions of the billet. To verify this theory, the porosity to helium was determined for the three locations in the large foam cylinders previously mentioned. This helium porosity would give a comparative value to determine the relative open cell or cell wall thickness. As the value of the helium porosity increases, the cell wall thickness would be thinner, with the possibility of an increase in open cell content. A helium-air pycnometer

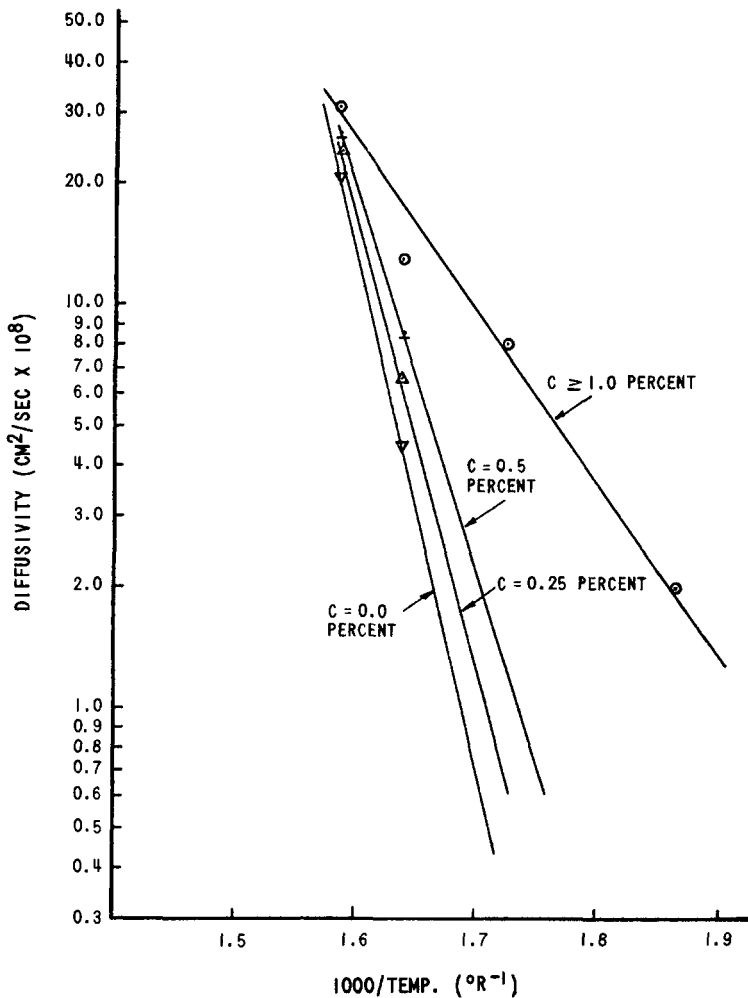


Fig. 9. Diffusivity as a function of temperature and concentration in 0.1 g/cm<sup>3</sup> foam.

(Micromeritics Instrument Corp., Model 1302) was used for these determinations. The results indicate that the foam samples from the center of the cylinder are 1.4 to 1.5 times as porous as the samples taken near the edges. The average helium porosity of three 1-in.<sup>3</sup> cylinders was reported as 51%, 41%, and 34% at the center, midpoint, and edge, respectively, for the 0.10 g/cm<sup>3</sup> foam. The same data for the 0.05 g/cm<sup>3</sup> foam was reported as 89%, 76%, and 63%. Similar results were obtained when air was used in place of helium.

This large variation in the helium and air porosity from the center to the outside edge of a large foam cylinder could account for a major part of the variation in the diffusivity between specimens. The higher porosity in the center is presumed to be due primarily to thinner cell walls. Thus, for a given density, more of the polymer would have to be located in the

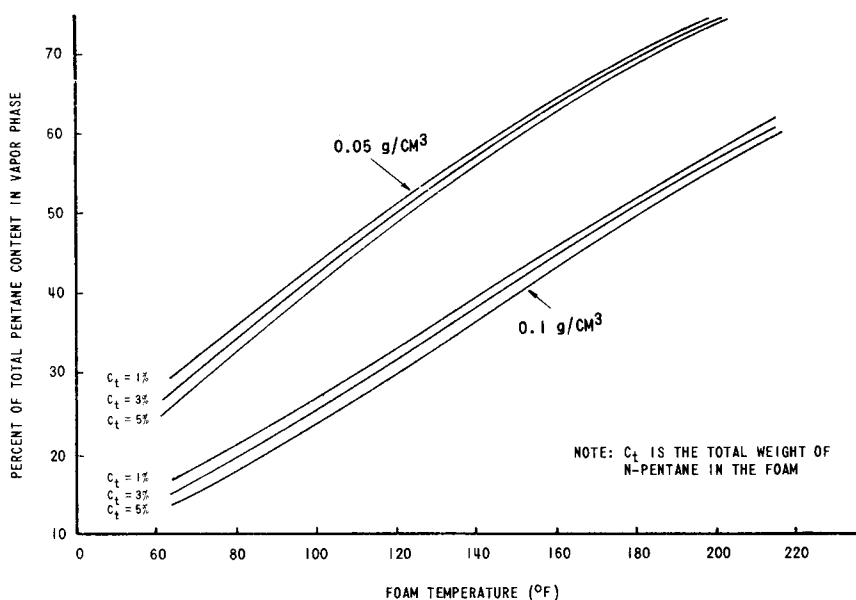


Fig. 10. Per cent of total *n*-pentane content located in vapor phase vs. temperature.

intersections of the cell walls near the center of the cylinders. Diffusion of gases through the intersections of the cell walls would be slow compared to the diffusion through the cell walls.

The porosity variation within the cylinder could have been caused by the method of molding the cylinders. The molding method involved heating the preexpanded beads to approximately 210°F (99°C), under a nitrogen pressure up to 80 psig (552 KN/m<sup>2</sup>) inside an autoclave. The pressure inside the beads would be 1 or 2 psi below the autoclave pressure during the molding operation due to nitrogen diffusing into the beads. When the pressure was quickly released from the autoclave, the beads expanded, filling the void space between the beads. The pressure in the beads was reduced slightly by the expansion of the beads. The foam cooled very slowly and the pressure slowly dissipated as the nitrogen diffused out of the foam. As a result, the foam near the center of the large cylinders remained at high temperature and pressure much longer than the foam near the edge. This high temperature and pressure may have caused thinner cell walls and ruptured some cell walls, causing the center to have higher porosity to helium and air.

The assumption of a uniform *n*-pentane concentration throughout the cylinders was also found to be untrue. From Figures 6 and 7, it can be seen that the slabs removed from the center of the cylinders had a lower initial *n*-pentane concentration  $C_0$  than the specimens removed from the edges of the cylinder. This *n*-pentane concentration gradient was also attributed to the molding process. The explanation for this *n*-pentane gradient was that the *n*-pentane, initially in a uniform distribution throughout the

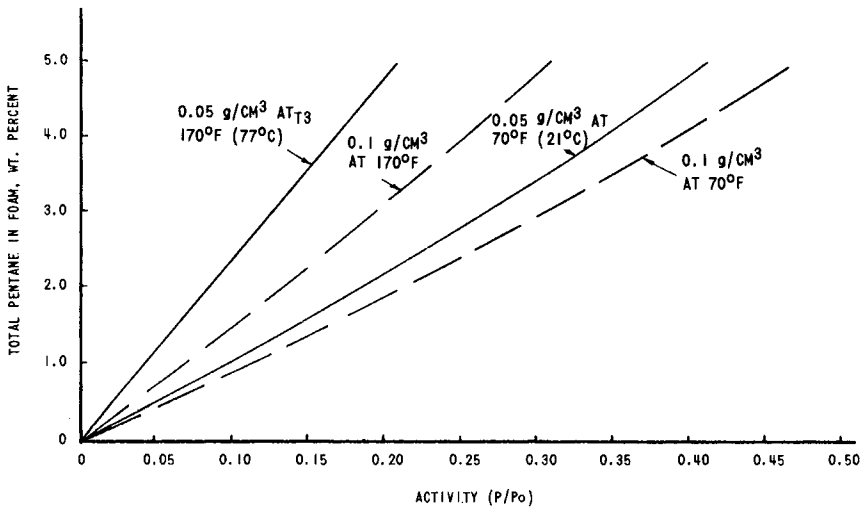


Fig. 11. Activity of *n*-pentane in polystyrene foam.

cylinder at the end of the molding cycle, started to migrate toward the outside because of a temperature gradient setup as the outside edges cooled down. When the *n*-pentane diffused to the colder section of the billet, more of it stayed in solution in the polystyrene resin, setting up a concentrations gradient in the vapor phase. With the steel mold wall around the major part of the cylinder and a lower diffusivity value, the diffusion of *n*-pentane out of the cylinder was drastically reduced. Thus, the *n*-pentane piles up around the edges of the cylinder. The major point of this explanation is the postulate that more of the *n*-pentane stayed in the polymer phase of the foam as the temperature of the foam decreased.

To determine the *n*-pentane distribution between the resin and vapor phase of the foam used in this investigation, the vapor pressure of the *n*-pentane in the vapor phase of the foam must be known. A computer program was used to calculate the equilibrium distribution of the *n*-pentane between the vapor phase and solid phase of the foam at any given temperature. The calculations were based on the ideal gas law and the Flory-Huggins equation. The Flory-Huggins equation<sup>2</sup> relates the vapor pressure of a solvent over a polymer-solvent solution. The resulting per cent *n*-pentane in the vapor phase for the two foam densities is shown in Figure 10. Additional data output from this computer program, the vapor pressure of *n*-pentane in the foam, and *n*-pentane activity at 70°F (21°C) and 170°F (77°C) are given in Figures 11 and 12, respectively.

The data in Figure 10 show that the per cent *n*-pentane in the vapor phase does decrease with decreasing temperature and is only slightly dependent upon total *n*-pentane concentration. Thus, the assumption made above, that more *n*-pentane is dissolved in the polymer at lower temperatures, was valid.



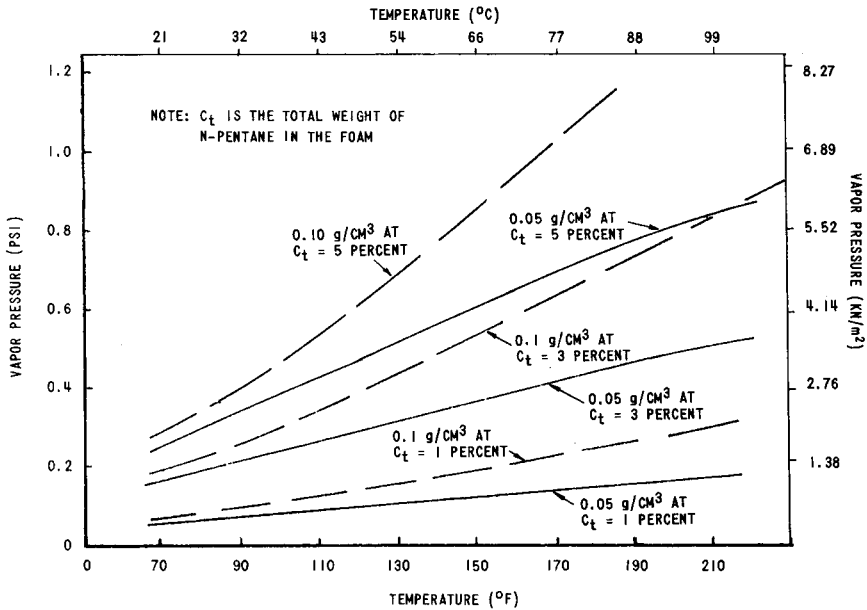


Fig. 12. Vapor pressure of *n*-pentane in polystyrene foam.

The diffusivity values determined in this investigation were used in an attempt to predict *n*-pentane profile in foam cylinders while aging at a constant temperature. Two foam cylinder sizes were considered: 36 in. in diameter by 25 in. high, and 1.129 in. in diameter by 1.000 in. high. The average *n*-pentane concentration was determined for these cylinders while they were being aged at four different temperatures.

The following assumptions had to be made to obtain the ideal diffusion model described earlier in this paper, although it has been shown that these assumptions do not apply in large cylinders:

1. The foam is homogeneous throughout, in that cell size, wall thickness, initial *n*-pentane concentration, and porosity are not a function of location.

2. The temperature is uniform and constant throughout the cylinder from the start of the aging cycle. No allowances were made for the time required to heat the cylinder from room temperature to the elevated aging temperature.

The calculated average *n*-pentane concentrations, as functions of aging time at given temperatures, are given in Figures 13 and 14. Foam cylinders, 0.05 g/cc and 0.10 g/cc, with an initial *n*-pentane concentration of 2.0% and the dimensions listed earlier, were used.

Figures 13 and 14 show that for the large-size cylinder (36 in. in diameter by 25 in. high), the average *n*-pentane concentration only decreased by about 0.4% in the 0.05 g/cm<sup>3</sup> foam and 0.3% in the 0.10 g/cm<sup>3</sup> foam after 200 days at 170°F (77°C). As would be expected, the average *n*-

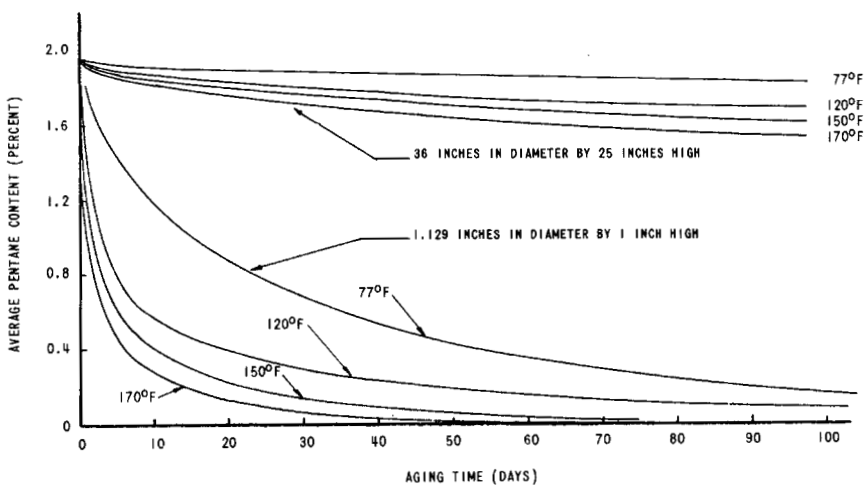


Fig. 13. Average *n*-pentane content in 0.05 g/cm<sup>3</sup> foam cylinders aging at constant temperature.

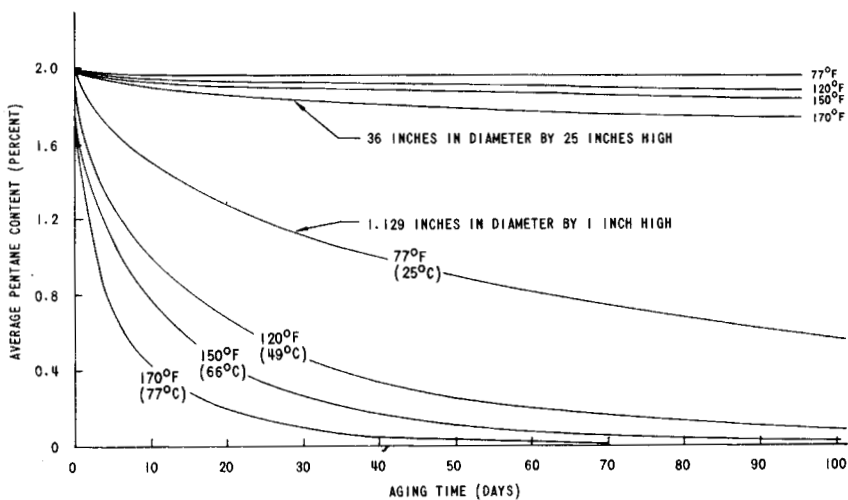


Fig. 14. Average *n*-pentane content in 0.1 g/cm<sup>3</sup> foam cylinders aging at constant temperature.

pentane concentration in the 1-in.<sup>3</sup> cylinders decreased at a much faster rate and approached 0% after 50 days at 170°F for each density.

In the case of the large cylinder, the predicted rate of *n*-pentane loss did not appear to be fast enough when compared to the *n*-pentane content data from actual foam cylinders of the same size that had been heat aged at 170°F (77°C) for 35 days. The *n*-pentane concentration drop in the large cylinder that had been heat aged was estimated to be 1.0% near the exterior and 0.5% in the center of the cylinder. This discrepancy between the predicted and actual *n*-pentane loss was attributed to the assumptions

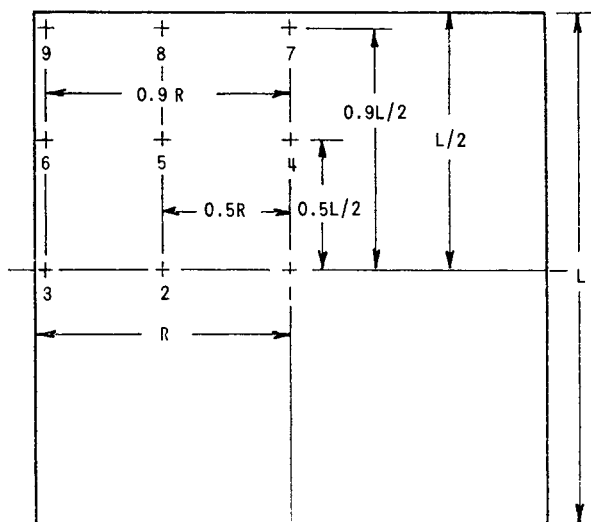


Fig. 15. Location of points in a foam cylinder for calculations of *n*-pentane shown on Figs. 16-19.

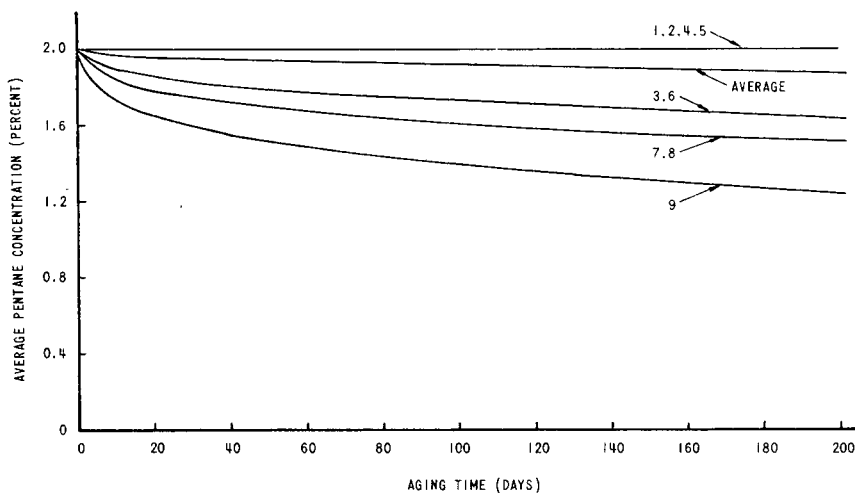


Fig. 16. *n*-Pentane distribution in a 36-in.-diameter by 25-in. high cylinder of 0.05 g/cm<sup>3</sup> foam aging at 77°F (25°C).

made in idealizing the diffusion model. As mentioned before, the foam was found to be nonhomogeneous in cell wall thickness and *n*-pentane concentration from the center of the cylinder to its outer regions as assumed in the diffusion model. With thinner cell walls and lower *n*-pentane concentration in the center of the cylinder, the *n*-pentane located in a region just inside the surface would initially diffuse inward and then outward. This would account for a faster drop in *n*-pentane concentration than was predicted by the ideal diffusion model.

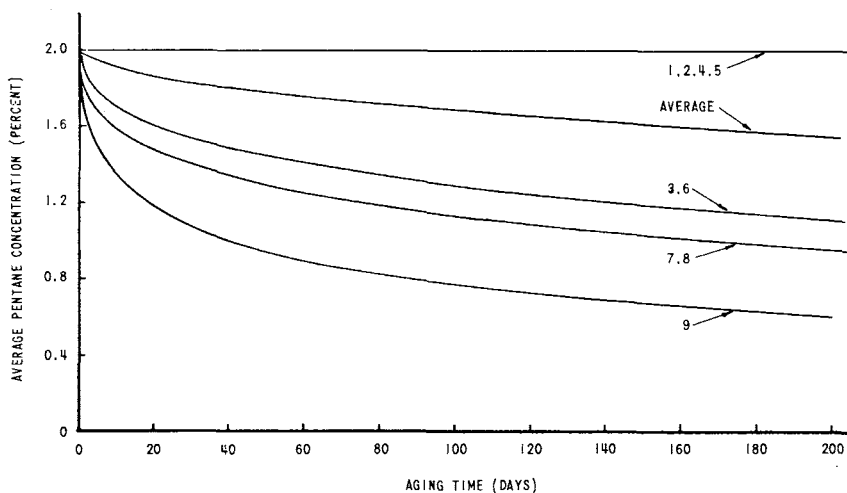


Fig. 17. *n*-Pentane distribution in a 36-in.-diameter by 25-in.-high cylinder of 0.05 g/cm<sup>3</sup> foam aging at 170°F (25°C).

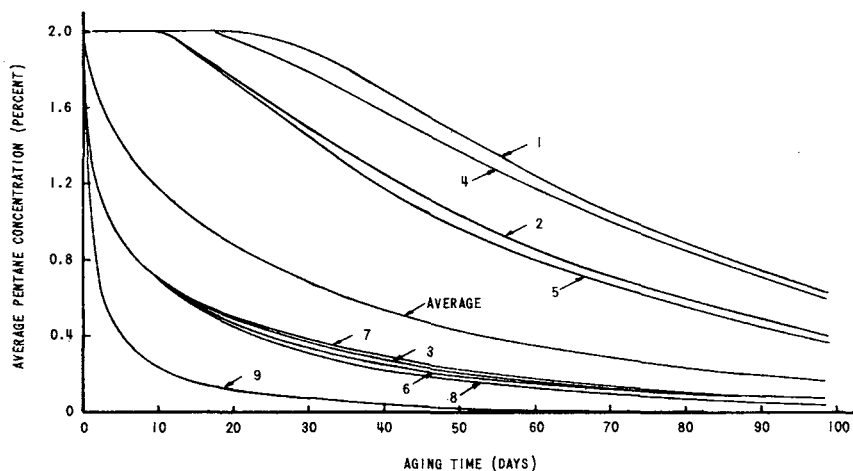


Fig. 18. *n*-Pentane distribution in a 1.129-in.-diameter by 1-in.-high cylinder of 0.05 g/cm<sup>3</sup> foam aging at 77°F (25°C).

The predicted *n*-pentane concentration in the 1-in.<sup>3</sup> cylinders was more consistent with data obtained from 1-in. cubes.<sup>1</sup> Comparing these data, allowing for the difference in shapes of the samples, the diffusion model predicted a *n*-pentane rate of loss a little greater than was reported for the 1-in. cubes. Thus, it appeared that the assumption of homogeneous material was valid for small cylinders.

The change in local *n*-pentane concentration at nine locations in  $\frac{1}{4}$  of a foam cylinder during aging at 77°F (25°C) and 170°F (77°C) was also calculated using the mathematical model previously described. The assumptions made for the average *n*-pentane concentration were used to

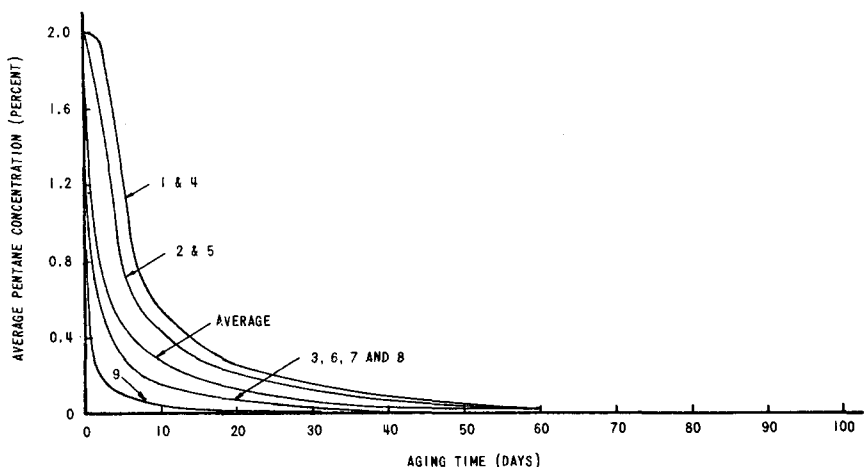


Fig. 19. *n*-Pentane distribution in a 1.129-in.-diameter by 1-in.-high cylinder of 0.05 g/cm<sup>3</sup> foam aging at 170°F (77°C).

obtain the ideal diffusion model. The results of the nine locations given in Figure 15 are shown on Figures 16 through 19. The average *n*-pentane concentrations calculated above are also as shown on these figures. There were no actual experimental data available for comparison. It may be noted, however, that the relative positions of the concentration lines for each location with the average concentration line were what one would expect. This was considered significant since the average *n*-pentane concentration was calculated from a different diffusion model. This was noted to be the case in all four examples shown.

In summary, ideal diffusion models developed for this investigation may be applied to homogeneous foam cylinders. However, when applying the models to nonhomogeneous foam, changes would have to be made to the models to predict accurately the rate of *n*-pentane loss. The *n*-pentane loss from foam shapes other than cylinders could also be predicted by making the necessary changes in the computer programs.

## CONCLUSIONS

The diffusivity of *n*-pentane through polystyrene bead foam can be predicted from weight loss-data.

The diffusivity of *n*-pentane through polystyrene bead foam has the magnitude of  $1 \times 10^{-8}$  to  $1 \times 10^{-6}$  cm<sup>2</sup>/sec and varies with temperature, foam density, *n*-pentane concentration, and foam structure.

The ideal diffusion models were developed which can be used to predict gas diffusion through foam.

The authors wish to thank Dr. Mark de Chazal (University of Missouri, Columbia), Dr. R. E. Skochdopole (Dow Chemical Co., Midland, Michigan), and Mr. Donald Hughes for their contributions to this work and to the Bendix Corporation, Kansas City Division, for allowing the publication of this work.

**References**

1. D. J. Fossey, Bendix Corporation, unpublished work.
2. J. Crank, *The Mathematics of Diffusion*, Oxford University Press, London, 1956.
3. R. E. Treybal, *Mass Transfer Operations*, McGraw-Hill, New York, 1955.

Received September 28, 1972

Revised November 21, 1972